

Production of Microcellular Polycarbonate Using Carbon Dioxide for Bubble Nucleation

V. Kumar
Assistant Professor

J. Weller
Graduate Student

Department of Mechanical Engineering,
University of Washington,
Seattle, Washington 98195

A process to produce a family of novel materials from polycarbonate, having a microcellular structure, is described. The process utilizes the high solubility of carbon dioxide in polycarbonate to nucleate a very large number of bubbles, on the order of 1 to 10×10^9 bubbles/cm³, at temperatures well below the glass transition temperature of the original, unsaturated polycarbonate. Microcellular polycarbonate foams with homogeneous microstructure and a wide range of densities have been produced. In this paper experimental results on solubility, bubble nucleation, and bubble growth in the polycarbonate-carbon dioxide system are presented, and the critical ranges of the key process parameters are established. It is shown that the bubble nucleation phenomenon in polycarbonate near the glass transition temperature is not described by classical nucleation theory.

Introduction

Microcellular plastics are composite materials made up of a polymer matrix and a large number of very small voids, typically 10^8 or more cells per cm³, with an average diameter on the order of $10 \mu\text{m}$. The concept of microcellular plastics was originally conceived by Suh (1979) as a means to reduce the amount of plastic used in mass produced items. The rationale was that if voids smaller than the critical flaws pre-existing in polymers can be created, then the material costs can be reduced while maintaining the necessary mechanical properties. The first microcellular foams were produced in high impact polystyrene by Martini et al. (1982, 1984), using nitrogen as the nucleating gas.

Microcellular plastics have the potential to significantly affect the way solid plastics are employed in a wide variety of applications. The small bubble size allows for foaming of thin-walled sections, in the 1 to 2 mm range, which are common in a number of consumer plastic items. Compared to solid polymers, microcellular polymers show promise of improving the fracture toughness as well; energy absorbed to fracture in tension tests were up to 400 percent higher for microcellular polystyrene compared to the unfoamed material (Waldman, 1982). Further, microcellular foams can be produced with an integral skin of desired thickness, composed of the solid polymer, allowing for the creation of a skin-core structure which can be tailored to provide the desired mechanical properties (Kumar and Weller, 1992).

The procedure to produce microcellular foam is a two stage batch process, as shown in Fig. 1. In the first stage, a polymer sample is saturated with a nonreactive gas maintained at an elevated pressure p_s for a time t_s which is sufficient to obtain a uniform concentration of gas in the polymer sample. The

gas saturation step is usually carried out at room temperature, although a higher temperature below the glass transition temperature of the polymer may be employed to speed up the gas

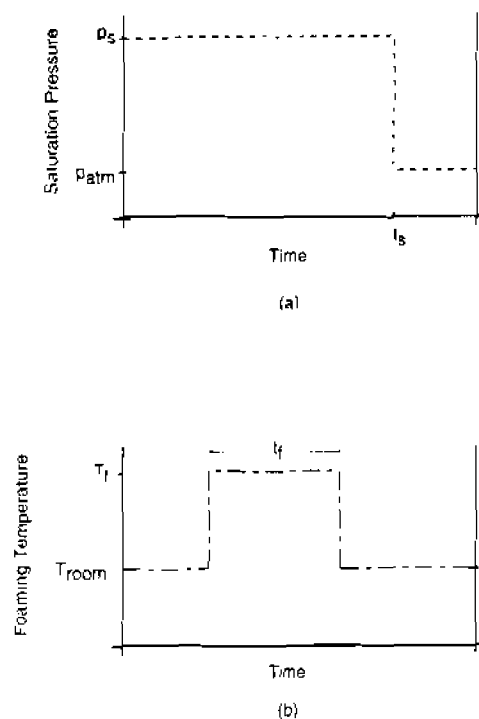


Fig. 1 Schematic of the microcellular process: (a) Stage I: polymer saturation at room temperature. (b) Stage II: bubble nucleation and growth at atmospheric pressure

Contributed by the Production Engineering Division for publication in the JOURNAL OF ENGINEERING FOR INDUSTRY. Manuscript received Nov. 1992; revised June 1993. Associate Technical Editor: S. Kapoor.

absorption process. When the pressure is released, a specimen supersaturated with gas is produced since the absorbed gas cannot readily escape from the polymer matrix. In the second stage, the supersaturated specimen is heated to the glass transition temperature T_g of the polymer, causing a large number of bubbles to nucleate and grow. Bubble growth occurs during the foaming time t_f . The relatively large polymer viscosity near the glass transition temperature limits bubble growth so that bubbles with diameters on the order of $10\ \mu\text{m}$ can be produced.

The majority of the work on microcellular foams to date has been conducted on the polystyrene-nitrogen system (Martini et al., 1982, 1984; Waldman, 1982; Kumar and Suh, 1990, Kumar, 1988; Colton and Suh, 1987). The microcellular structure has also been produced in other thermoplastics, including PVC (Kumar and Weller, 1992), PET (Kumar and Gebizlioglu, 1991; Baldwin and Suh, 1992) and styrene-butadiene (Ramesh et al., 1992). Recently, Park and Youn (1992) have successfully used ultrasonic excitation to achieve bubble nucleation in Polyol resin supersaturated with nitrogen to create polyurethane foams. This novel method of activating bubble nucleation, as opposed to the direct heating of supersaturated polymer samples employed by Martin et al. (1984), represents an interesting development towards the synthesis of a continuous process to produce microcellular foams.

As polycarbonate is a widely used engineering thermoplastic, creation of a microcellular structure in polycarbonate is of special interest. Martini et al. (1984) produced microcellular polystyrene foams with void fractions in the 5 to 30 percent range using nitrogen as the nucleating gas. We chose carbon dioxide as the nucleating gas due to its high solubility in polycarbonate. An order of magnitude more bubbles nucleated than in the polycarbonate- CO_2 system than in the polystyrene- N_2 system. As a result, we were able to produce microcellular foams with void fractions up to 90 percent potentially offering a much wider range of mechanical properties to the engineer.

Experimental

Commercially available polycarbonate sheets of approximately 1.5 mm thickness were used in the experiments. The original, unsaturated material had a density of $1.2\ \text{g}/\text{cm}^3$ and a glass transition temperature of 150°C . Samples approximately $25\text{mm} \times 25\text{mm}$ were cut from the sheets, and placed in a pressure vessel connected to a carbon dioxide cylinder. The pressure within the vessel was regulated using a single stage regulator, and the gas sorption was carried out at room

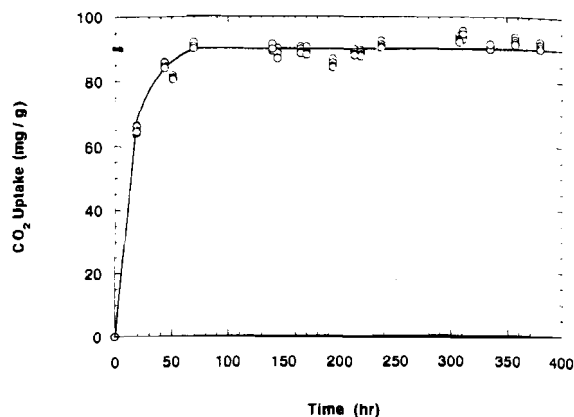


Fig. 2 Plot of carbon dioxide uptake at 4.8 MPa (700 psi) and 22°C in polycarbonate as a function of time

temperature which varied between 20 and 25°C , with an average of 22°C . The amount of gas absorbed by the samples was monitored by periodically weighing them on a precision balance with an accuracy of 10 micrograms. Because the amounts of CO_2 absorbed were on the order of milligrams, this weighing method provided sufficient accuracy for monitoring gas content in the polymer samples. For the 1.5mm thick samples used in this experiment, the time required for saturation was approximately 70 hours (see Fig. 2).

Upon saturation the samples were removed from the pressure vessel and brought to atmospheric conditions. The samples were then placed in a glycerin bath maintained at the foaming temperature T_f for a length of time t_f , also referred to as the foaming time. Immediately after the samples were removed from the glycerin bath, they were quenched in room temperature water. To study the internal microstructure, the samples were placed in liquid nitrogen for several minutes and then fractured. The fractured surface was made conductive by deposition of Au-Pd vapor and studied under a scanning electron microscope (SEM). All micrographs were taken at the center of the sample.

Determination of Cell Size and Density. Observations of micrographs of microcellular foams produced by unconstrained foaming in a heated bath show fewer and relatively larger bubbles near the surface, and a higher density of smaller bubbles in the core region (Kumar, 1988). Thus the bubble

Nomenclature

A = area of the micrograph, cm^2
 C = gas concentration at saturation, cm^3 (STP) per gram of polymer
 C_0 = concentration of gas molecules, molecules/ cm^3
 D = diffusivity, cm^2/sec
 f_0 = frequency factor for gas molecules joining the nucleus, sec^{-1}
 H = Henry's law constant for the gas-polymer system, cm^3 (STP)/ gPa
 k = Boltzman's Constant, J/K
 l = sample thickness, cm
 M = magnification factor of the micrograph

M_d = molecular weight of the diluent
 M_p = molecular weight of the monomer
 n = number of bubbles in a micrograph
 N_f = number of bubbles per cm^3 of foam
 N_{HOM} = homogeneous nucleation rate, cells/ $\text{cm}^3\ \text{sec}$
 N_0 = number of bubbles nucleated per cm^3 of original unfoamed polymer
 p_0 = environmental pressure, Pa
 p_s = gas saturation pressure, Pa
 R = gas constant
 t = saturation time, sec

t_f = foaming time, sec
 t_s = saturation time, hr
 T = foaming temperature, K
 T_g = reduced glass transition, $^\circ\text{C}$
 T_{g0} = glass transition of the pure polymer, $^\circ\text{C}$
 V_f = the volume occupied by the voids in one cm^3 of foam
 z = coordination number
 ΔC_{pp} = excess transition isobaric specific heat of the polymer, $\text{cal}/\text{g}^\circ\text{C}$
 $\Delta G'$ = activation energy, J
 γ = surface energy of the polymer, J/m
 ω = mass fraction of diluent

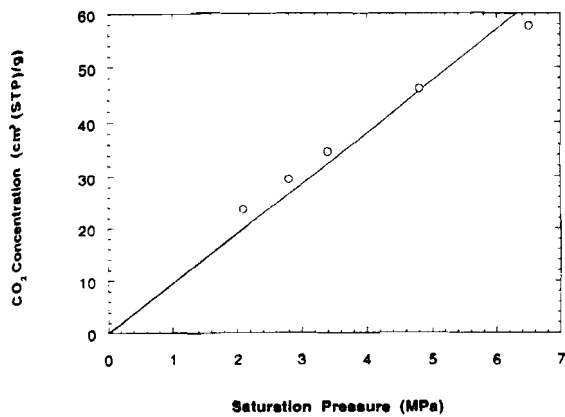


Fig. 3 Plot of equilibrium carbon dioxide concentration in polycarbonate as a function of saturation pressure. Experiments were conducted at room temperature.

density can change with position across the specimen thickness. To quantify the bubble density at a given location, we first define the number of bubbles per cm³ in the foam N_f . The N_f is then corrected by the local void fraction V_f to obtain the number of bubbles nucleated per cm³ of the original, unfoamed polymer, N_0 . Defining the bubble nucleation density with reference to the unfoamed polymer allows one to compare the nucleation densities achieved under different processing conditions.

N_f , V_f , and N_0 are estimated from the scanning electron micrographs according to the following procedure. First a micrograph showing 100 to 200 bubbles is obtained, and the number of bubbles, n , in the micrograph is determined. If A is the area of the micrograph in cm² and M is the magnification factor, then $(n/A/M^2)$ gives the area bubble density or the number of bubbles per cm² of the foam. Assuming an isotropic bubble distribution, the square root of the area density gives a line-density or the number of bubbles per cm of the foam. By cubing the line density, the number of bubbles per cm³ of the foam, N_f , can be estimated

$$N_f = \left(\frac{nM^2}{A} \right)^{3/2} \quad (1)$$

A second micrograph at a higher magnification is obtained at the same location in the sample as the first micrograph, so that the average bubble diameter D can be determined. Because many bubble diameter measurements can be made on a single micrograph, the mean and standard deviation of the bubble diameter can be determined. In our experiments, the major and minor diameters of approximately 25 bubbles were measured in each of these micrographs. After determining the average bubble diameter, the volume occupied by the voids in one cm³ of foam V_f can be estimated as

$$V_f = \left(\frac{\pi}{6} \right) D^3 N_f \quad (2)$$

and the volume occupied by the polymer in one cm³ of foam is therefore approximated by $(1 - V_f)$. Thus N_f bubbles in one cm³ of the foam must have nucleated in $(1 - V_f)$ cm³ of the original polymer. Therefore, the number of bubbles nucleated per cm³ of original unfoamed polymer N_0 can be estimated from

$$N_0 = \frac{N_f}{(1 - V_f)} \quad (3)$$

The cell density reported in this paper is given by Eq. (3). Note that, in this procedure, we are likely to underestimate the average bubble diameter since the fracture surface will most likely not pass through a diametral plane for every bubble in

the micrograph. Hence the local void fraction V_f , as well as the bubble density N_0 , are underestimated by Eqs. (2) and (3), respectively. There are established methods to make statistical and stereographic corrections to the average bubble diameter determined from a micrograph (see, for example, Underwood, 1970). However, these corrections were not applied to the data reported in this paper, as our main purpose was to establish a qualitative understanding of the key process variables.

Experimental Results

Solubility of Carbon Dioxide in Polycarbonate. The amount of gas dissolved in a polymer is given by Henry's law (Durril and Grisley, 1969)

$$C = H p_s \quad (4)$$

where

C = gas concentration at saturation, cm³ (STP) per gram of polymer

H = Henry's law constant for the gas-polymer system, cm³ (STP)/g Pa

p_s = gas saturation pressure, Pa

Figure 2 shows carbon dioxide uptake in mg of CO₂ per gram of polycarbonate as a function of sorption time for five polycarbonate samples placed under 4.83 MPa (700 psi) carbon dioxide at room temperature. The limiting solubility is seen to be approximately 90 mg/g, or 9 percent by weight at this pressure, reached in approximately 70 hours. This experiment was repeated at a number of gas saturation pressures. Figure 3 shows the equilibrium concentration in units of cm³ (STP) per gram of polycarbonate as a function of the saturation pressure. We can see that the equilibrium gas concentration increases linearly with the gas saturation pressure, as predicted by Eq. (4). Thus carbon dioxide sorption obeys Henry's Law in polycarbonate for the range of saturation pressures explored. From the experimental data, the Henry's Law constant for the polycarbonate-CO₂ system was determined to be 9.5×10^{-6} cm³ (STP)/g Pa.

Effect of Saturation Pressure on Cell Nucleation. Colton and Suh (1987a, 1987b) have suggested that bubbles in the microcellular process may nucleate either homogeneously or heterogeneously. Heterogeneous nucleation occurs when a second phase is present in the polymer due to an insoluble additive or a nucleation agent. Homogeneous nucleation occurs when a sufficient number of dissolved gas molecules come together for a long enough time to produce a stable bubble nucleus. In the polycarbonate used in this study, there were no nucleating agents used, so the expected nucleation mechanism is homogeneous nucleation for which the rate of nucleation has been proposed by Colton and Suh (1987a) as

$$N_{HOM} = C_0 f_0 \exp(-\Delta G^{**}/kT) \quad (5)$$

where

N_{HOM} = number of bubbles nucleating/cm³ sec

C_0 = concentration of gas molecules, molecules/cm³

f_0 = frequency factor for gas molecules joining the nucleus, sec⁻¹

k = Boltzman's Constant, J/K

T = temperature, K

ΔG^{**} = activation energy, J

The activation energy for homogeneous nucleation is approximated by (Colton and Suh, 1987b)

$$\Delta G^{**} = \frac{16\pi\gamma^3}{3(p_s - p_0)^2} \quad (6)$$

where

γ = surface energy of the polymer, J/m²

p_s = gas saturation pressure, Pa

p_0 = environmental pressure, Pa

Table 1 Summary of experimental conditions and results at different saturation pressures with foaming temperature and foaming time held constant at 150°C and 10 sec, respectively

Sample	p_s (MPa)	$N_0 \times 10^{-9}$ (cells/cm ³)	Bubble Diameter		Foam Density (g/cm ³)	CO ₂ Concentration (mg/g)
			Average (μ m)	Standard Deviation (μ m)		
a1	2.1	0.19	11.03	2.75	0.76	46.6
a2	2.1	0.28	9.53	2.18	0.77	45.9
b1	2.8	1.1	8.75	2.70	0.55	58.0
b2	2.8	1.5	8.51	2.99	0.50	60.4
c1	3.4	1.8	6.85	1.72	0.50	68.2
c2	3.4	2.1	8.86	2.25	0.50	67.0
c3	3.4	1.9	7.82	2.28	0.55	68.1
d	4.8	9.5	5.08	1.60	0.47	90.6
e1	6.5	28.9	3.45	0.96	0.46	113.2
e2	6.5	25.6	3.30	1.01	0.48	112.2

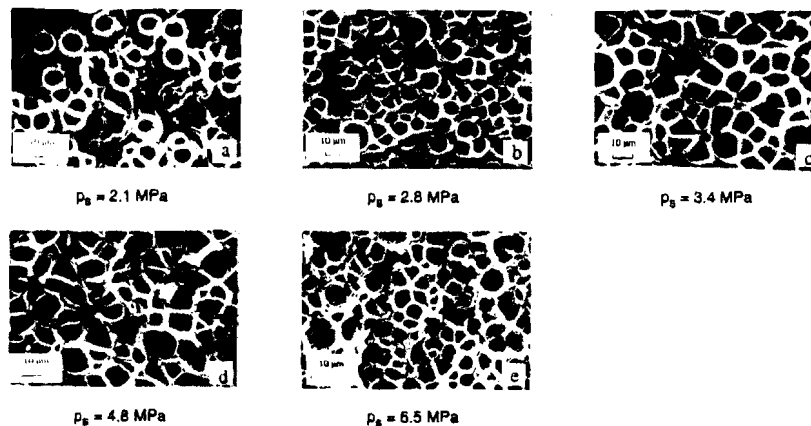


Fig. 4 Scanning electron micrographs of polycarbonate samples saturated with carbon dioxide at different pressures. The samples were foamed at 150°C for 10 sec (see Table 1).

The effect of gas saturation pressure on the cell nucleation density can be qualitatively seen from Eqs. (5) and (6). Equation (6) shows that a higher saturation pressure leads to a lower activation energy which causes a higher nucleation rate. Therefore, a higher gas saturation pressure leads to a higher cell nucleation density.

Polycarbonate samples were saturated with carbon dioxide at various pressure ranging from 2.07 MPa (300 psi) to 6.55 MPa (950 psi) at 22°C. The samples were foamed at 150°C for 10 seconds and then examined under a scanning electron microscope. Table 1 summarizes the experimental conditions, the average cell sizes and the cell nucleation densities determined from the micrographs.

Figure 4 shows SEM micrographs of samples that were saturated at different CO₂ pressures and foamed under the conditions noted above. It is evident that more bubbles nucleate and the average bubble diameter gets smaller as the gas saturation pressure is increased. The cell nucleation density has been plotted on a log scale in Fig. 5 as a function of the gas saturation pressure. For the range of saturation pressures explored in these experiments, we can say that the number of cells nucleated increases exponentially with the gas saturation pressure. Figure 6 shows a comparison of the measured cell nucleation density and homogeneous nucleation theory, Eq. (5). The value used for f_0 , the frequency factor for gas molecules joining the nucleus, is given by Colton and Suh (1987), and is on the order of 10⁻³/sec. The concentration of gas molecules, C_0 , is a function of the saturation pressure, and is given by Henry's Law, Eq. (4). The foaming temperature used was 150°C ($T=323$ K), and the surface energy of the polymer

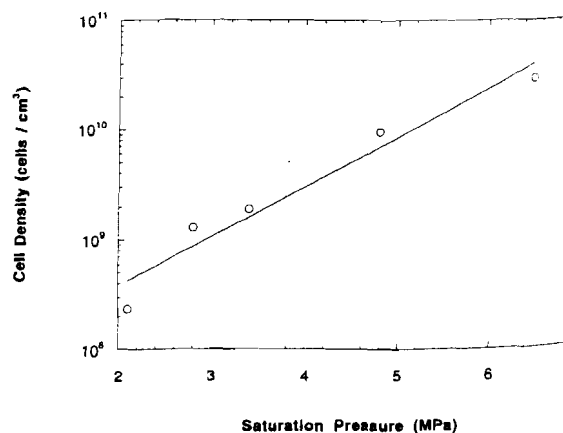


Fig. 5 Plot of bubble nucleation density as a function of carbon dioxide saturation pressure. Sample were foamed for 10 sec at 150°C.

at the foaming temperature is 35.6×10^{-3} J/m² (Brandrup and Immergut, 1989). Finally, the nucleation rate is multiplied by the length of time during which bubbles are nucleating. A value of 1.0 sec was used following the procedure of Colton and Suh (1987). We see from Fig. 6 that the homogeneous nucleation theory does not agree with the experimental data. For example, a gas pressure of 60 MPa is needed to nucleate 10⁹ bubbles/cm³ according to the model, yet we observe 10⁹ bubbles/cm³ at a far lower saturation pressure of 3 MPa.

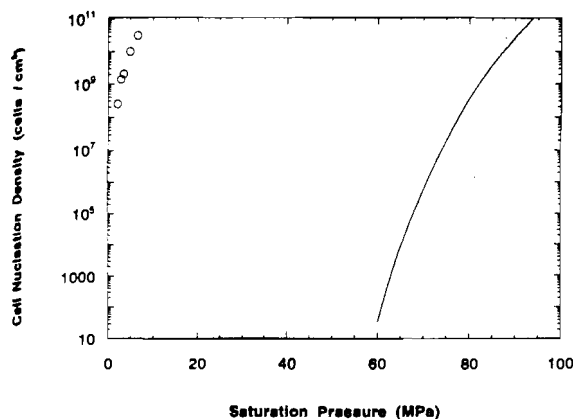


Fig. 6 Comparison of the measured bubble nucleation density shown in Fig. 5 and the homogeneous nucleation theory

An alternative nucleation mechanism has been proposed by Kweeder et al. (1991) which does not rely on the classical nucleation theories. The model assumes a log-normal distribution of extremely small microvoids in the polymer matrix. The nucleation density is calculated by determining which microvoids within the initial distribution are large enough to survive as stable nuclei. The theory predicts substantial nucleation at the saturation pressures used in the microcellular process, a significant improvement over homogeneous theory. However, this model uses a prescribed size distribution of microvoids, and the mean and standard deviation of the distribution are tuned to fit the experiment. Although this approach represents an improvement over the classical nucleation model there is, as yet, no confirmation of the existence of microvoids or the assumed size distribution.

The average cell diameter has been plotted in Fig. 7 as a function of the gas saturation pressure. The data in Fig. 5 represents an average from 25 to 50 bubbles, and the error bars represent one standard deviation at each condition. Note that the bubble size decreases nearly linearly as the gas saturation pressure is increased. This may at first be counter-intuitive, since at higher saturation pressures there is more gas in the sample which is able to support cell growth. The bubble size, however, is intimately related to the number of cells that nucleate. As the cell nucleation density increases (see Fig. 5), more bubbles compete for the available gas volume, and the average cell diameter decreases. This behavior was first noted in microcellular polystyrene by Kumar (1988), and has been predicted by other authors (Arefmanesh et al., 1992a).

Effect of Foaming Temperature on Cell Nucleation. The original microcellular process (Martini et al., 1984) heated supersaturated thermoplastic sheets to the glass transition temperature of the original, unsaturated material to cause cell nucleation and growth. However, because of the high concentration of gas in the polymer, significant plasticization occurs, resulting in a lower glass transition temperature. A theoretical model has been developed to predict the glass transition in polymer-diluent systems by Chow (1980), and has been shown to be in good agreement with experimental data (Chiou et al., 1985). According to this model, the glass transition temperature is given by

$$\ln\left(\frac{T_g}{T_{g0}}\right) = \beta[(1-\theta)\ln(1-\theta) + \theta\ln(\theta)]$$

where

$$\beta = \frac{zR}{M_p \Delta C_{pp}} \quad (8)$$

$$\theta = \frac{M_p \omega}{z M_d (1-\omega)} \quad (9)$$

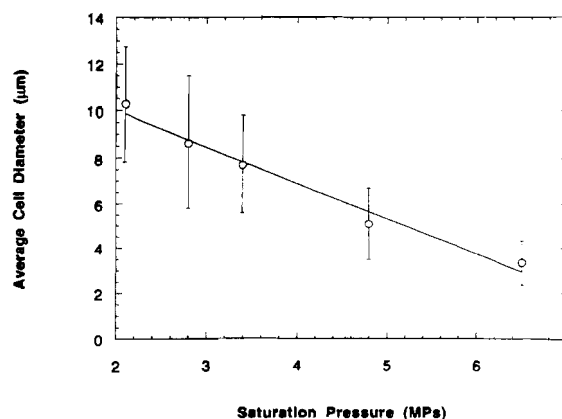


Fig. 7 Plot of average cell diameter as a function of carbon dioxide saturation pressure. Samples were foamed for 10 sec at 150°C.

- ω = mass fraction of diluent,
- M_p = molecular weight of the monomer,
- M_d = molecular weight of the diluent,
- R = gas constant,
- T_{g0} = glass transition of the pure polymer,
- T_g = reduced glass transition,
- z = coordination number,
- ΔC_{pp} = excess transition isobaric specific heat of the polymer.

For polycarbonate, Chiou et al. (1985) suggests a $\Delta C_{pp} = 0.0585 \text{ cal/g}^\circ\text{C}$. The glass transition of the pure polycarbonate used in this experiment was 150.0°C, and M_p is 254 g/mol. In addition, Chow (1980) recommends a value of $z = 2$, based on comparison with experimental data. From Fig. 3 we can see that for a saturation pressure of 4.8 MPa (700 psi), the concentration of CO_2 is approximately 90 mg/g, thus $\omega = 0.090$. Using the above values, the glass transition temperature of polycarbonate, saturated with a CO_2 concentration of 90 mg/g is calculated from Eq. (7) to be 87°C. We therefore expected that bubble nucleation in polycarbonate saturated with carbon dioxide may occur at temperatures significantly below 150°C, the T_g of unsaturated polycarbonate.

To investigate the effect of foaming temperature on cell nucleation, samples were foamed at successively lower temperatures, starting at 160°C, for a period of 30 seconds in the glycerin bath. The lowest temperature at which cell nucleation was observed in this experiment was 60°C. Figure 8 shows SEM micrographs of foamed samples from this experiment, arranged in the order of increasing foaming temperatures (60 to 160°C). Figure 8 shows that there is cell nucleation at temperatures substantially below the glass transition temperature of the original material, confirming a significant increase in the mobility of the polymer due to carbon dioxide sorption. Note that the cell nucleation density in micrographs, *a*, *b*, and *c* of Fig. 8 appears to be nonhomogeneous. The cells have nucleated along certain lines, like beads on a string. This behavior is in marked contrast with the behavior modeled by the homogeneous nucleation theory.

The cell nucleation density has been plotted in Fig. 9 as a function of the foaming temperature. We see that the cell nucleation density lies between 1 and $5 \times 10^9 \text{ cells/cm}^3$ over the entire 100°C range of foaming temperatures used, and shows no particular trend with respect to foaming temperature. To a first approximation, the number of cells nucleated can be considered to be independent of the foaming temperature. This insensitivity of the cell nucleation density to increases in the foaming temperature is very striking, for if the bubble nucleation process has an Arrhenius-type dependence on temperature as suggested by classical nucleation theory, Eq. (5), then reducing the foaming temperature from 160 to 60°C should reduce the number of bubbles nucleated by approximately three

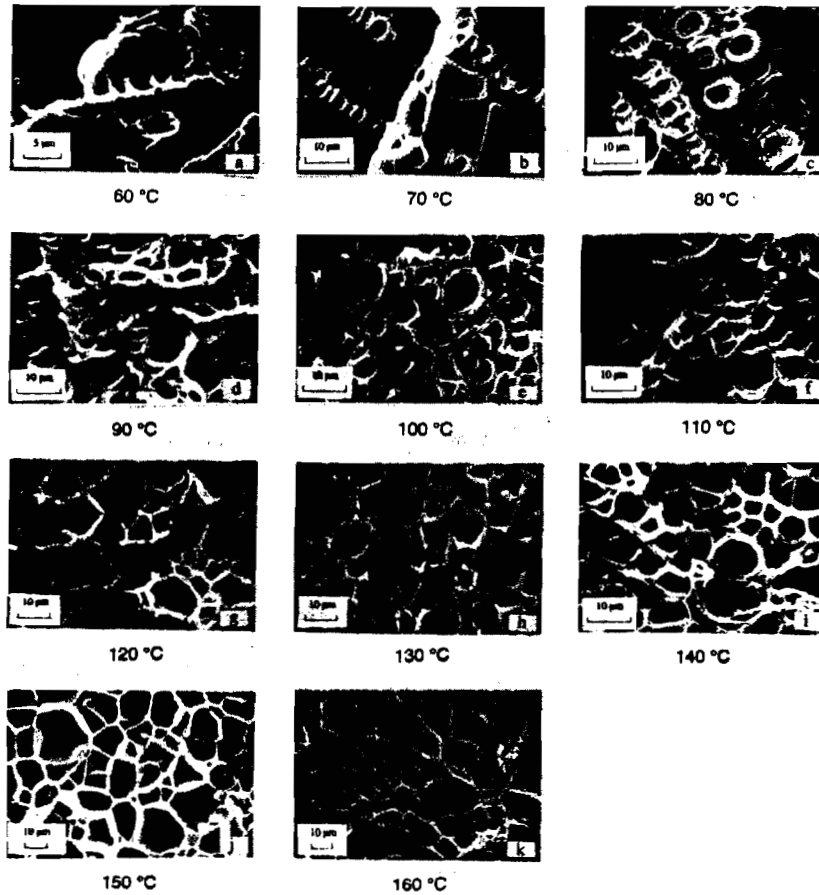


Fig. 8 Scanning electron micrographs of polycarbonate samples foamed at different temperatures. The samples were saturated at 4.8 MPa (700 psi) and foamed for 30 sec (see Table II).

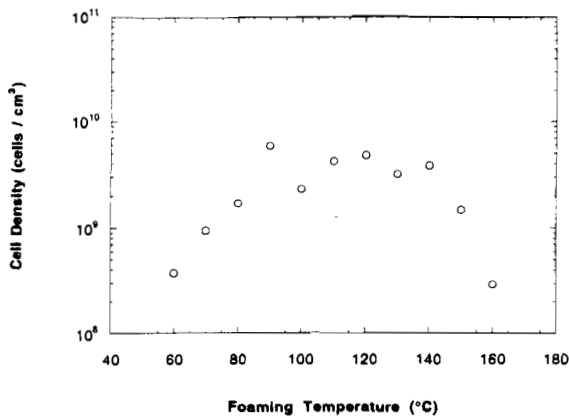


Fig. 9 Plot of bubble nucleation density as a function of foaming temperature. Samples were saturated at 4.8 MPa (700 psi) and foamed for 30 sec.

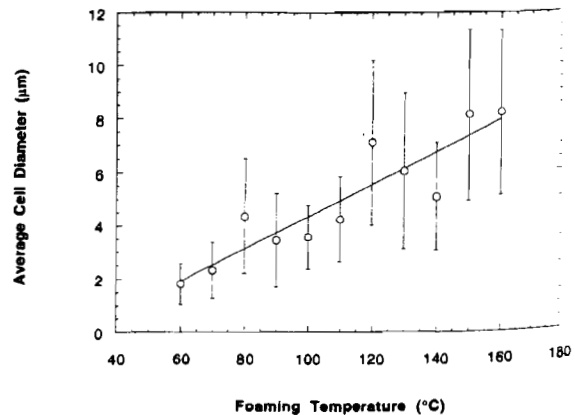


Fig. 10 Plot of average bubble diameter as a function of foaming temperature. Samples were saturated at 4.8 MPa (700 psi) and foamed for 30 sec.

orders of magnitude. Once again, we find that the classical nucleation theory does not describe the observed data even in a qualitative way.

In Fig. 10, the average cell diameter as a function of foaming temperature has been plotted. As expected, the cell size increases with increasing foaming temperature, which has been predicted by Arefmanesh et al. (1992b). Figure 11 shows the foam density as a function of foaming temperature. The foam density decreases monotonically with temperature, which is consistent with a relatively constant cell nucleation density and

an increase in the average bubble diameter with temperature. It is worth noting that at 160°C, a foam has been produced with a density of 0.1 g/cm³, representing a 90 percent reduction in density relative to unfoamed polycarbonate. In addition, the cells, on the average, are below 10 μm in diameter. Thus, it is possible to create low density polycarbonate foams having a microcellular structure by nucleating a very large number of bubbles.

Bubble Growth with Time. The rate at which bubbles grow with time at a particular foaming temperature is an important

process parameter. This rate is a function of the gas concentration available for growth, the polymer viscosity and surface tension, and the pressure inside the bubbles at a given instant

Table 2 Summary of experimental conditions and results at different foaming temperatures with saturation pressure and foaming time held constant at 4.8 MPa and 30 sec, respectively

Sample	Foaming Temp. (°C)	$N_0 \times 10^{-9}$ (cells/cm ³)	Bubble Diameter		Foam Density (g/cm ³)
			Average (μm)	Standard Deviation (μm)	
a	60.0	0.36	1.81	0.77	1.21
b	70.0	0.91	2.31	1.04	1.08
c	80.0	1.7	4.34	2.15	1.02
d	90.0	5.6	3.45	1.75	0.92
e	100.0	2.3	3.56	1.20	0.84
f	110.0	4.1	4.23	1.59	0.75
g	120.0	4.1	7.11	3.08	0.66
h	130.0	3.0	6.05	2.91	0.53
i	140.0	3.7	5.08	2.01	0.37
j	150.0	1.3	8.14	3.20	0.25
k	160.0	0.26	8.21	3.09	0.11

Table 3 Summary of experimental conditions and results at different foaming times with saturation pressure and foaming temperature held constant at 4.8 MPa and 150°C, respectively

Sample	Foaming Time (sec)	$N_0 \times 10^{-9}$ (cells/cm ³)	Bubble Diameter		Foam Density (g/cm ³)
			Average (μm)	Standard Deviation (μm)	
a	5.0	4.3	5.12	1.62	0.72
b	10.0	3.2	6.15	1.81	0.49
c	20.0	2.3	6.97	2.83	0.32
d	130.0	1.3	8.14	3.20	0.25
e	40.0	1.6	9.86	4.09	0.22
f	60.0	2.5	8.66	3.13	0.17
g	90.0	1.8	10.32	3.92	0.15
h	120.0	0.71	13.13	4.61	0.15
i	240.0	0.95	9.71	4.44	0.18

of time The pressure inside the bubbles in turn changes as the bubbles grow, and is affected by the rate at which gas molecules diffuse into the bubbles from the surrounding polymer.

To establish the rate of cell growth, a number of samples were saturated at 4.83 MPa (700 psi) and foamed for different lengths of time at a foaming temperature of 150°C. The resulting structure was studied under a scanning electron microscope. The experimental conditions for the samples as well as the resulting cell nucleation density, cell size, and density of the foam are summarized in Table 3.

Figure 12 shows SEM micrographs of foamed samples, arranged in the order of increasing foaming time, ranging from 5 sec for sample (a) to 4 minutes for sample (i). Note that the distance between bubbles, which is approximately 2 μm in sample (a), decreases as the bubbles grow. Beyond 10 seconds of foaming, sample (b), the bubbles begin to interfere with each other, and as growth progresses, the general structure changes from spherical bubbles to cells with a polyhedral shape. Bubbles also coalesce as growth proceeds, as shown by occasional bubbles several times larger than their neighbors (see for example, the top left corner of sample (i)).

The average bubble diameter has been plotted in Fig. 13 as a function of foaming time. The bubbles are observed to grow

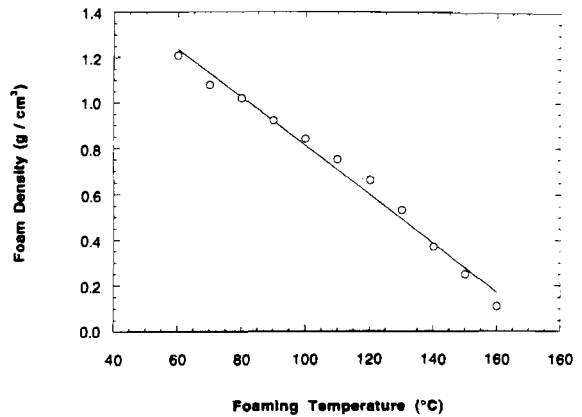


Fig. 11 Plot of foam density as a function of foaming temperature. Samples were saturated at 4.8 MPa (700 psi) and foamed for 30 sec.

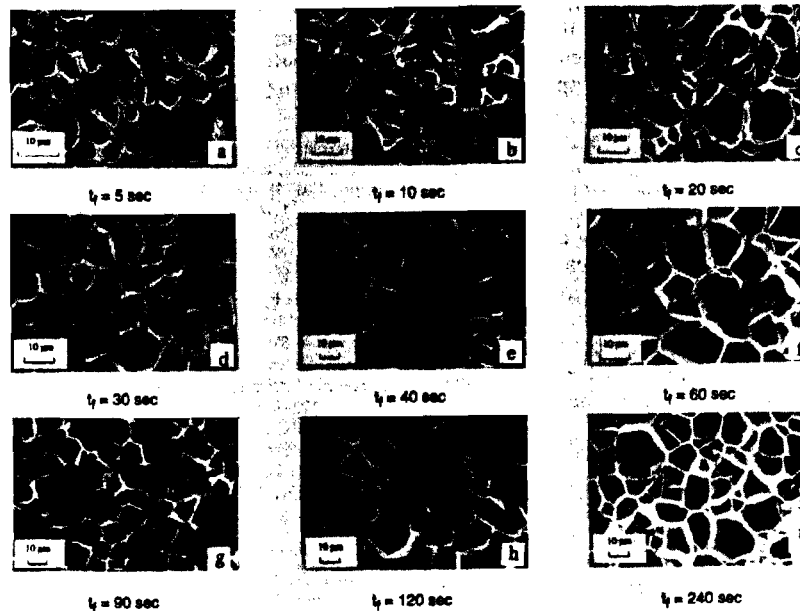


Fig. 12 Scanning electron micrographs of polycarbonate samples foamed at 150°C for different lengths of time. The samples were saturated at 4.8 MPa (700 psi) (refer to Table 3).

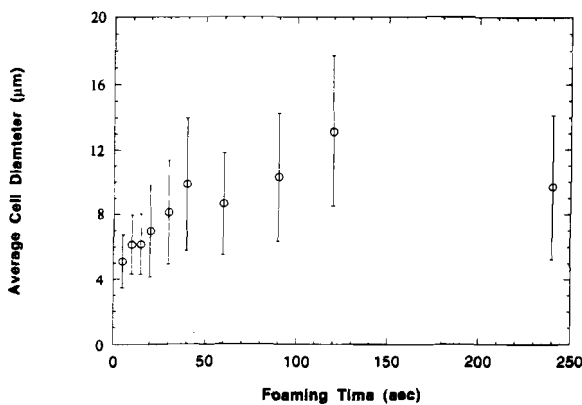


Fig. 13 Plot of average bubble diameter as a function of foaming time. Samples were saturated at 4.8 MPa (700 psi) and foamed at 150°C.

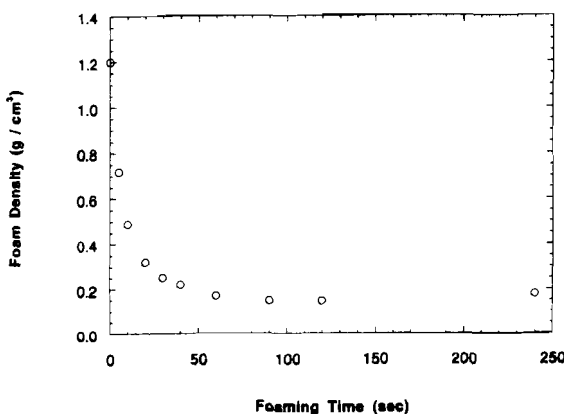


Fig. 14 Plot of foam density as a function of foaming time. Samples were saturated at 4.8 MPa (700 psi) and foamed at 150°C.

rapidly at first, and then at a decreasing rate until finally the driving force for bubble growth has been depleted and a stable structure has been attained. An important observation from Fig. 13 is that nearly half of the eventual cell diameter is achieved in the first 10 to 15 seconds of growth. The structure appears to stop growing after approximately 100 seconds of foaming. In Fig. 14 the foam density has been plotted as a function of foaming time. The foam density appears to reach a steady state after approximately 100 seconds, which is consistent with the observations from Fig. 13 on bubble growth.

Concluding Remarks

The microcellular structure was successfully created in polycarbonate using carbon dioxide as the nucleating gas. Cell nucleation densities in the range of $1 - 10 \times 10^9$ per cm^3 can be achieved, allowing for the synthesis of polycarbonate foams with densities as low as 10 percent of the density of original polymer. The foam density was found to vary linearly with foaming temperature, allowing for simple yet accurate control of this important foam property.

Microcellular nucleation in the polycarbonate- CO_2 system can be achieved at temperatures well below the glass transition temperature of the original material due to a lowering of the glass transition temperature by the plasticizing effect of absorbed carbon dioxide. Bubble nucleation was observed at 60°C, which is 90°C below the glass transition temperature of the original polymer. Our success in introducing a new structure in the polymer under the influence of a very high con-

centration of gas molecules, approximately 10 percent of gas by weight in the polymer, may lead to a new way of processing polymers and of changing their structure.

The classical bubble nucleation theories are not applicable to the nucleation mechanisms in polymers near the glass transition temperature. In the foaming temperature range 60-160°C, the bubble nucleation density was found to be essentially independent of temperature, which is in marked contrast with the Arrhenius-type temperature dependence for nucleation rates predicted by the classical theories of nucleation. Similarly, the experimental data on cell nucleation density as a function of gas saturation pressure was found to be many orders of magnitude away from predictions based on the homogeneous nucleation theory. Thus, new theoretical approaches are needed to describe the bubble nucleation phenomena in the microcellular process.

Acknowledgments

This research was supported by National Science Foundation Grants DDM 8909104 and MSS 9114840, and a grant from the Washington Technology Centers. This support is gratefully acknowledged.

References

- Arefmanesh, A., Advani, S. G., Michaelides, E. E., 1992a, "Accurate Numerical Solution for Mass Diffusion-Induced Bubble Growth in a Viscous Fluid Containing Limited Dissolved Gas," *International Journal of Heat and Mass Transfer*, Vol. 35, pp. 1711-1722.
- Arefmanesh, A., and Advani, S. G., 1992b, "Non-Isothermal Bubble Growth in Polymeric Foams," *Cellular Polymers*, ASME MD-Vol. 38, pp. 25-40.
- Baldwin, D. F., and Suh, N. P., 1992, "Microcellular Poly(ethylene terephthalate) and Crystallizable Poly(ethylene terephthalate): Characterization of Process Variables," *SPE Technical Papers*, Vol. 38, pp. 1503-1507.
- Brandrup, J., and Immergut, E. H., 1989, *Polymer Handbook*, 3rd edition, John Wiley & Sons, NY, p. VI/420, 433.
- Chiou, J. S., Barlow, J. W., and Paul, D. R., 1985, "Plasticization of Glassy Polymers by CO_2 ," *Journal of Applied Polymer Science*, Vol. 30, pp. 2633-2642.
- Chow, T. S., 1980, "Molecular Interpretation of the Glass Transition Temperature of Polymer-Diluent Systems," *Macromolecules*, Vol. 13, pp. 362-364.
- Colton, J., and Suh, N. P., 1987, "Nucleation of Microcellular Foam with Additives: Part I: Theoretical Considerations," *Polymer Engineering and Science*, Vol. 27, pp. 485-493.
- Durril, P. L., and Grisley, R. G., 1969, "Diffusion and Solubility of Gases in Thermally Softened or Molten Polymers," *AIChE Journal*, Vol. 15, pp. 106-110.
- Kumar, V., and Weller, J. E., 1992, "Creating an Integral, Unfoamed Skin on Microcellular Foams," *SPE Technical Papers*, Vol. 38, pp. 1508-1512.
- Kumar, V., 1988, "Process Synthesis for Manufacturing Microcellular Thermoplastic Parts," Ph.D. Thesis, Department of Mechanical Engineering, Massachusetts Institute of Technology, Cambridge, MA.
- Kumar, V., and Gebizlioglu, O. S., 1991, "Carbon Dioxide Induced Crystallization in PET Foams," *SPE Technical Papers*, Vol. 37, pp. 1297-1299.
- Kumar, V., and Suh, N. P., 1990, "A Process for Making Microcellular Thermoplastic Parts," *Polymer Engineering & Science*, Vol. 30, pp. 1323-1329.
- Kumar, V., and Weller, J. E. 1992, "Microcellular PVC," *SPE Technical Papers*, Vol. 38, pp. 1508-1510.
- Kweeder, J. A., Ramesh, N. S., Campbell, G. A., and Rasmussen, D. H., 1991, "The Nucleation of Microcellular Polystyrene Foam," *SPE Technical Papers*, Vol. 37, pp. 1398-1400.
- Martini J. E., Suh, N. P., and Waldman, F. A., 1984, US Patent No. 4,473,665.
- Martini, J. E., Waldman, F. A., and Suh, N. P., 1982, "The Production and Analysis of Microcellular Thermoplastic Foams," *SPE Technical Papers*, Vol. 28, pp. 674-676.
- Park, H., and Youn, J. R., 1992, "Processing of Cellular Polyurethane by Ultrasonic Excitation," *ASME JOURNAL OF ENGINEERING FOR INDUSTRY*, Vol. 114, pp. 323-328.
- Ramesh, N. S., Kweeder, J. A., Rasmussen, D. H., and Campbell, G. A., 1992, "An Experimental Study of the Nucleation of Microcellular Foams of High Impact Polystyrene," *SPE Technical Papers*, Vol. 38, pp. 1078-1081.
- Suh, N. P., 1979, Personal Communication with Professor Nam P. Suh, Department of Mechanical Engineering, Massachusetts Institute of Technology, Cambridge, MA.
- Underwood E. E., 1970, *Quantitative Stereology*, Addison-Wesley Publishing Company, Reading, MA.
- Waldman, F. A., 1982, "The Processing of Microcellular Foam," S. M. Thesis, Department of Mechanical Engineering, Massachusetts Institute of Technology, Cambridge, MA.